Journal of Magnetic Resonance Open 23 (2025) 100195

Contents lists available at ScienceDirect

Journal of Magnetic Resonance Open

journal homepage: www.sciencedirect.com/journal/journal-of-magnetic-resonance-open

Ultrafast 2D benchtop NMR spectroscopy enhanced by flow Overhauser dynamic nuclear polarization

Joris Mandral [a,1], Johnnie Phuong [b,c,1], Jonathan Farjon [a], Patrick Giraudeau [a], Kerstin Münnemann [b,c,*], Jean-Nicolas Dumez [a,*]

[a] Nantes Université, CNRS, CEISAM UMR6230, F-44000, Nantes, France
[b] Laboratory of Engineering Thermodynamics (LTD), RPTU Kaiserslautern D-67663, Kaiserslautern, Germany
[c] Laboratory of Advanced Spin Engineering – Magnetic Resonance (LASE-MR), RPTU Kaiserslautern D-67663, Kaiserslautern, Germany

ARTICLE INFO

Keywords:
Overhauser DNP
Ultrafast NMR
Flow NMR

ABSTRACT

Benchtop Nuclear Magnetic Resonance (NMR) spectroscopy is a powerful analytical technique for the monitoring of reactions and processes due to its accessibility and lower cost compared to high-field NMR. However, benchtop NMR spectroscopy often suffers from limited sensitivity and resolution. In this work, we have combined ultrafast (UF) 2D NMR with Overhauser Dynamic Nuclear Polarization (ODNP) to tackle both problems. Compared to thermally polarized 1D NMR, UF 2D NMR provides improved spectral resolution in a single scan whereas ODNP boosts the NMR sensitivity. To demonstrate the possibility of combining UF 2D NMR with ODNP for process monitoring applications, experiments were carried out at different flow conditions. Our results show that ODNP at least compensated for the losses in sensitivity of UF 2D NMR that are normally induced by high flow velocities. Moreover, under certain flow conditions, ODNP brings additional sensitivity to UF 2D NMR spectra, with SNR increased by a factor of >3 compared to thermal equilibrium acquisitions. The methods developed in this article are expected to be beneficial for more informative and sensitive acquisitions in the context of process monitoring.

1. Introduction

Process analytical technologies are crucial for the process industry, allowing reactions and processes to be understood and reaction parameters to be optimized to achieve better yields and selectivities [1–3]. NMR spectroscopy is a powerful analytical technique for process monitoring because it provides continuous, non-invasive structural and quantitative analysis of the molecules involved in a reaction [4–6]. Benchtop NMR spectrometers are ideal for this task, due to their mobility and low cost compared to high-field NMR spectrometers [7–12]. There are numerous examples in the literature where benchtop NMR spectroscopy has been applied to a biological or a chemical process in a bypass setup, emphasizing the advantages of this technology for online monitoring applications [13–20].

However, process monitoring using benchtop NMR spectrometers faces two major limitations [21], which arise from their limited magnetic field strength: (i) low sensitivity and (ii) the complexity of classical 1D ^{1}H NMR spectra, which leads to peak overlap and difficulties in peak assignment as well as quantitative analysis. Both aspects contribute to limiting the complexity of the samples, the concentrations range and the reachable timescales that can be addressed in monitoring applications using benchtop NMR spectrometers. In continuous-flow applications, these problems are particularly severe due to the limited premagnetization volume and flow-induced NMR signal broadening.

Several methods have been developed to deal with the complexity of 1D ^{1}H NMR spectra of mixtures measured on benchtop NMR instruments. Besides the possibility to study the mixture with heteronuclei, e.g. with ^{13}C NMR spectroscopy, 2D NMR spectroscopy is an elegant solution. In recent years, fast 2D NMR techniques have emerged that allow signal acquisition on a timescale that is suitable for process monitoring. These techniques include 2D NMR experiments based on non-uniform sampling (NUS) strategies, techniques with fast repetition methods with shorter recovery times between consecutive scans, and ultrafast (UF) 2D NMR methods based on spatial encoding [22–25]. Among these methods, UF 2D NMR offers the most significant acceleration, providing a complete 2D NMR spectrum in a single scan of less

* Corresponding authors.
E-mail addresses: kerstin.muennemann@mv.uni-kl.de (K. Münnemann), jean-nicolas.dumez@univ-nantes.fr (J.-N. Dumez).
[1] co-first authors

https://doi.org/10.1016/j.jmro.2025.100195

Available online 10 March 2025

than one second (as opposed to several minutes with conventional methods) [26]. Examples of the successful applications of UF 2D NMR (especially 2D UF COSY) can be found in the literature [27–33]. However, the spatial parallelization process on which UF 2D NMR relies on results in a sensitivity penalty. This adds to the general sensitivity problem of benchtop NMR spectroscopy, which can be alleviated by the use of hyperpolarization methods.

Hyperpolarization methods can boost the sensitivity of NMR spectroscopy and are therefore promising techniques for reaction and process monitoring [34,35]. Among these, two techniques have been shown to be suitable for continuous hyperpolarization of flowing samples: Signal Amplification By Reversible Exchange (SABRE) [36–39] and Overhauser Dynamic Nuclear Polarization (ODNP) [40–44]. Compared to SABRE, ODNP is especially well suited for process monitoring applications because ODNP can be applied to a wide range of molecules, is technically simple, and can work in continuous-flow [45]. The usage of immobilized radicals on a fixed bed enables the flow-induced separation of the radicals from the measured liquid before NMR detection. In addition, ODNP has already been coupled to benchtop NMR spectrometers, enhancing benchtop ^{1}H as well as ^{13}C NMR spectroscopy of mixtures [44,46–48]. However, examples of benchtop NMR spectroscopy with ODNP have been mostly limited to the use of 1D NMR methods.

In this work, we demonstrate the possibility to combine the acquisition of UF 2D NMR spectra with the signal enhancement provided by ODNP for the analysis of a mixture on a benchtop NMR spectrometer. To the best of our knowledge, this is the first study that reports on this interesting option. To demonstrate the feasibility of the method, homonuclear ^{1}H correlation spectroscopy (COSY) of a mixture hyperpolarized by ODNP was conducted with the UF 2D NMR method. The 2D NMR spectra of a binary hyperpolarized mixture of propionaldehyde and 1,3-dioxane were acquired in continuous-flow as well as interrupted-flow at different flow rates. The results of both flow modes were compared with each other and the effects of the set flow rate as well as the advantages of the flow modes are discussed.

2. Experimental procedure

2.1. Chemicals and materials

An equimolar mixture of 1,3-dioxane (TCI Chemicals, purity > 98 %) and propionaldehyde (Thermo Scientific, purity > 99 %) was prepared gravimetrically using a laboratory scale (Delta Range XS603S, Mettler Toledo, accuracy: ± 0.001*g*). For hyperpolarization, a fixed-bed with immobilized radicals was used [45]. The radical glycidyl-oxy-tetramethylpiperidinyloxyl (GT) was grafted on an aminopropyl-functionalized controlled porous glass (CPG) which has a pore size of 30 nm. GT was attached to the CPG via a polyethylene-imine linker (molecular mass: 25,000 g.mol^{-1}) and an intermediate linker consisting of 1,4-butanediol diglycidyl ether.

2.2. Setup and experimental procedure

The setup consists in a custom-built Halbach magnet (magnetic field strength 0.35 T), which contained the custom-built ODNP probe, and a Magritek benchtop NMR spectrometer (Spinsolve Carbon, magnetic field strength 1.0 T). The setup is illustrated in Fig. 1. The studied mixture, provided in a feed container, was pumped (WADose Plus HP, Flusys, accuracy: < 3 %) to the ODNP probe, passing a 6-port valve (Rheodyne 7030, IDEX). PEEK capillaries were connected to the 6-port valve so that the setup could be operated in both continuous-flow as well as in interrupted-flow mode (controlled by a custom written LabView program). The ODNP probe contained the flow cell (inner diameter 1 mm) in which the paramagnetic radical matrix was packed as dense fixed-bed. ODNP hyperpolarization was conducted at a microwave

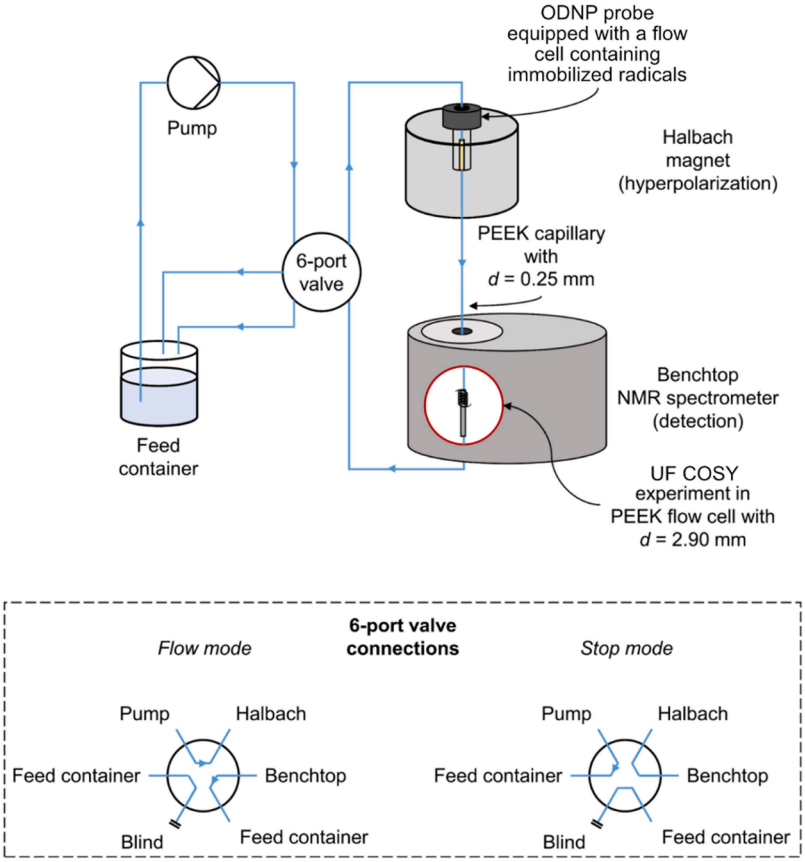

Fig. 1. Scheme of the experimental setup for the 2D UF COSY experiments with ODNP hyperpolarization in continuous-flow and interrupted-flow.

frequency of 9.687 GHz and a power of 10 W. After hyperpolarization, the sample was transported by a PEEK capillary (inner diameter 0.25 mm, length 0.52 m) to the benchtop NMR spectrometer, which was placed directly under the Halbach magnet. The benchtop NMR spectrometer was equipped with a detection cell with an inner diameter of 2.9 mm. Additional details regarding the experimental setup may be found in refs [45,48].

All NMR experiments were controlled by the Spinsolve Expert software (Magritek).

2D COSY NMR spectra were acquired with the ultrafast acquisition method and are referred to as 2D UF COSY. The 2D UF COSY experiments were acquired using 100 pairs of consecutive bipolar gradients. Each gradient duration is 1150 μs with an amplitude of ± 14.4 G.cm^{-1}. A gradient resting delay of 530 μs is also applied between consecutive acquisition gradients. A dwell time of 10 μs was used to cover a frequency range larger than the frequency dispersion induced by the gradient pulses. The total duration of the EPSI (Echo-Planar Spectroscopic Imaging) is 336 ms. Two 15 ms chirp pulses were used together with ± 2.4 G.cm^{-1} gradients for spatial encoding. These parameters resulted in a spectral width of 294 Hz in the direct/conventional dimension and 340 Hz in the indirect/UF dimension. The detailed UF COSY pulse sequence is available in the Supporting Information (see Figure.S1).

2D UF COSY experiments with ODNP hyperpolarization were carried out in both continuous-flow and interrupted-flow modes. Corresponding 2D UF COSY experiments without ODNP hyperpolarization were additionally performed to enable the calculation of the signal enhancements. The performance and the quality of the experiments in continuous-flow as well as interrupted-flow were assessed at three flow rates in the transport capillary (or flow velocities calculated by assuming plug-flow). For the 2D UF COSY experiments, the acquisitions were synchronized to the ODNP hyperpolarization build-up in the Halbach magnet and the transport to the detection zone depending on the chosen flow rate. In interrupted-flow mode, the switch of the 6-port valve was synchronized to that delay time as well, and the NMR acquisition was launched simultaneously. The three different flow rates, flow velocities and the corresponding transport times are summarized in the following Table 1. The transport time delays were determined in preliminary experiments detailed in the Supporting Information (see Fig.S2).

The corresponding 1D thermal as well as 1D ODNP experiments were conducted as well. The 1D ^{1}H NMR spectra were acquired with a single scan and 32,768 data points with a dwell time of 200 μs, resulting in spectral width of 5 kHz. Inversion recovery experiments were conducted as well for the site-specific determination of the T1 times of the propionaldehyde/1,3-dioxane mixture and are provided in the Supporting Information (see Table.S1).

2D UF COSY NMR spectra were processed using custom written programs in MATLAB (Mathworks). The postprocessing routine was carried out as follows: half of the echoes (odd echoes) were reorganized into a 2D matrix. Along the spatial dimension, the data were inverse Fourier transformed, apodized with a Gaussian window, zero-filled and Fourier transformed. Along the spectral dimension, the data were apodized with a sine window, zero-filled and Fourier transformed. Magnitude spectra were used in all cases.

The data were then analyzed using Mnova (Mestrelab) for plotting and signal-to-noise ratios (SNR) measurements. The calculation of the signal enhancements was done by SNR measurements of each individual signal. For each experimental condition, the enhancements factors were determined by dividing the SNRs between the corresponding signals of ODNP hyperpolarized spectra and the thermally polarized spectra. This procedure was repeated three times since three consecutive experiments were conducted for each experimental condition. Then the average enhancement factors were calculated as well as their standard deviation over the three repetitions. The detailed enhancements factors are detailed in the Supporting Information (Table S2). All the experiments were repeated 3 times to calculate average enhancement values as well as standard deviations.

Table 1
Summary of the three flow rates in the transport capillary (in mL.min^{-1}), the corresponding flow velocities in the capillary (in m.s^{-1}), and the corresponding transport times of the flowing mixture.

Flow rates (mL.min^{-1})	Flow velocities in the capillary (m.s^{-1})	Transport time (s)
1	0.34	6
3	1.02	4
5	1.70	2

3. Results and discussion

3.1. NMR characterization of the model mixture

In order to characterize the combination of flow ODNP and UF 2D NMR, we selected a 50:50 mixture propionaldehyde/1,3-dioxane, which are expected to be polarized by ODNP at 0.35 T. Fig. 2 shows the 1D ^{1}H NMR spectrum and the corresponding 2D UF COSY NMR spectrum of the equimolar mixture of propionaldehyde/1,3-dioxane as well as the peak assignments, both acquired at thermal equilibrium and static conditions. As shown in Fig. 2(a), the 1D ^{1}H NMR spectrum of the mixture displays five signals with different multiplicities. The 2D UF COSY NMR spectrum, given in Fig. 2(b) allows clear distinction of the two spin systems by revealing cross-peaks. In total, there are 9 signals: 5 located on the diagonal and 4 cross-peaks due to the homonuclear coupling.

3.2. UF COSY in continuous-flow vs. interrupted-flow at thermal equilibrium

Fig. 3 shows the results of the 2D UF COSY experiments which were conducted without ODNP hyperpolarization in continuous-flow and interrupted-flow at different flow rates. UF 2D NMR relies on a spatial parallelization process, which is susceptible to disturbances due to diffusion and flow [49]. At the same time, sample motion is intrinsic to both the ODNP experiment and to flow NMR monitoring. Therefore, we first studied the effect of the flow conditions on UF 2D NMR acquisitions, without hyperpolarization. 2D UF COSY spectra were acquired at thermal equilibrium using either continuous-flow or interrupted-flow mode. In the continuous-flow approach, the flow rate remains unchanged between transport and NMR acquisition.

For the 2D UF COSY experiments acquired in continuous-flow, it can be recognized that the quality of the spectra significantly decreases with increasing flow rate. In UF 2D NMR, both spatial encoding and spatially-resolved acquisition require several tens of milliseconds. During this delay, the continuous-flow induces a displacement of the ^{1}H spins, which can be detrimental to the quality of the resulting spectrum, depending on the direction of the displacement relative to that used for spatial encoding [50,51]. In this case, the coil used for spatial encoding produces a field gradient that is transverse, i.e., orthogonal to the direction of the net sample displacement. However, the geometry of the flow cell results in a jet flow and thus velocities that do have transverse components, resulting in the observed attenuation [52,53]. It is in fact remarkable that good-quality spectra can still be obtained at such flow velocity (0.34 m.s^{-1} in the transport capillary).

In contrast, 2D UF COSY NMR spectra with good quality are obtained when the interrupted-flow mode is applied. The results are consistent for all flow rates and are comparable to the spectra which were acquired of samples at rest. This observation can be attributed to the fact that the sample motion is stopped sufficiently fast preventing the interference with the acquisition during the 2D UF COSY experiment However, SNR decrease by applying a 5 mL.min^{-1} flow rate. For the 2D UF COSY experiments in interrupted-flow, the average SNR of the nine signals drops from 31 to 25 when the flow rate is changed from 1 mL.min^{-1} to 5 mL.

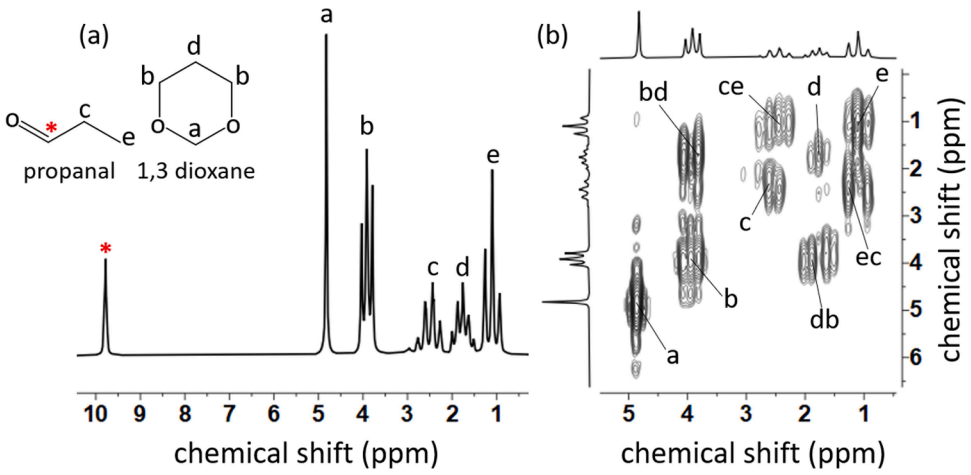

Fig. 2. **(a)** 1D ^{1}H NMR spectrum of the equimolar mixture of propionaldehyde and 1,3-dioxane with peak assignments. **(b)** 2D UF COSY NMR spectrum of the 50:50 mixture of propionaldehyde and 1,3-dioxane with peak assignments. Both NMR spectra were acquired at thermal equilibrium and in static conditions. The aldehyde proton (indicated by a red cross) was discarded in this work, as a spectral width of 10 ppm cannot be achieved for the 2D UF COSY experiments with the current setup.

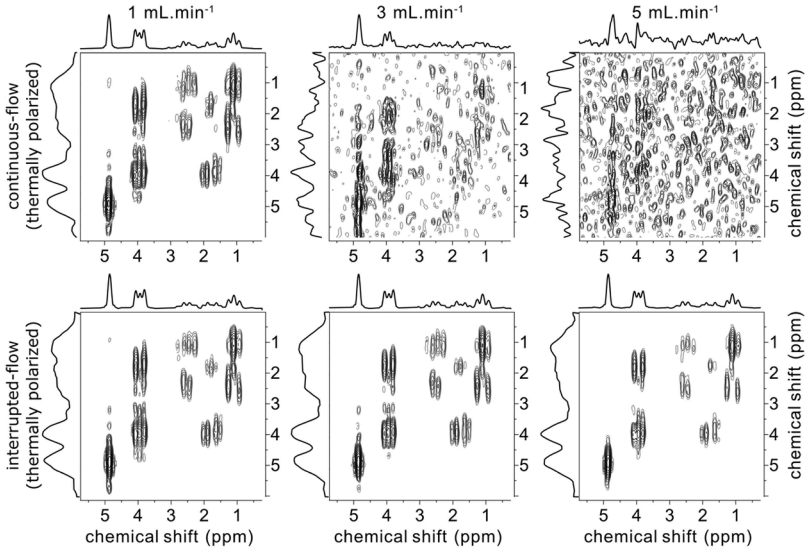

Fig. 3. Thermally polarized 2D UF COSY NMR spectra of the equimolar mixture of propionaldehyde an 1,3-dioxane at a flow rate of 1, 3 and 5 mL.min^{-1}. Top: 2D UF COSY NMR spectra acquired in continuous-flow mode. Bottom: 2D UF COSY NMR spectra acquired in interrupted-flow mode.

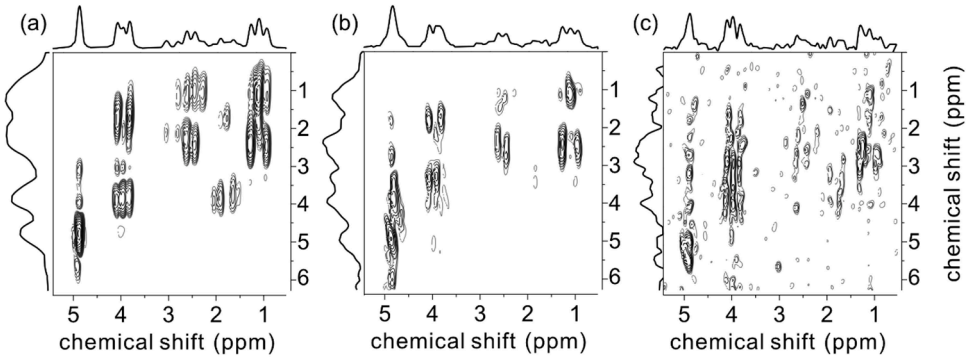

Fig. 4. 2D UF COSY NMR spectra of an equimolar mixture of propionaldehyde and 1,3-dioxane at **(a)** 1 mL.min^{-1}, **(b)** 3 mL.min^{-1} and **(c)** 5 mL.min^{-1}, enhanced by ODNP hyperpolarization in continuous-flow mode.

min^{-1}. This is due to insufficient premagnetization occurring at high flow velocities. For comparison with the transport times, the T_1 values are provided in the Supporting Information (see Table. S1). In the following, the corresponding 2D UF COSY experiments with ODNP hyperpolarization are discussed in detail. The signal enhancements in the 2D UF COSY spectra and the beneficial effects by ODNP are explicitly shown.

3.3. UF COSY + ODNP in continuous-flow

2D UF COSY experiments with ODNP hyperpolarization were carried out in continuous-flow. The results of the equimolar mixture of propionaldehyde and 1,3-dioxane for the different flow rates are given in Fig. 4. The acquisition of UF COSY spectra for the ODNP-hyperpolarized mixture was first attempted using continuous-flow acquisition. In this approach, the sample is flowing continuously, the microwaves are turned on and a UF 2D NMR spectrum is acquired when the polarization has reached a plateau in the detection cell. The delay (transport time) between turning on the microwave and acquiring the spectrum was optimized using prior 1D experiments described in the Supporting Information (see Figure S2).

As observed in the studies without ODNP hyperpolarization, good quality 2D UF COSY NMR spectra are again obtained for a flow rate of 1 mL.min^{-1}. By applying ODNP hyperpolarization, the SNR of the nine signals is significantly improved. The average signal enhancement by ODNP is $\varepsilon = \mathbf{2.51 \pm 0.24}$. 1D ^{1}H acquisitions under the same flow conditions show an average signal enhancement of $\varepsilon = \mathbf{7.02 \pm 0.57}$ when ODNP is applied, which is much higher, but still in the same order of magnitude. SNR enhancements of the 1D NMR experiments conducted in continuous-flow are provided in the Supporting Information (Figure S3). For comparison, the enhancement factors measured in the Halbach Magnet (for ODNP) are in the order of 30–40, demonstrating that there is a substantial loss of polarization during the transfer of the sample, and also due to the formation of a jet flow in the detection cell and corresponding backmixing effects. These effects are in detail described in [48] where the same setup has been used. In contrast, the 2D UF COSY NMR spectra obtained at flow rates of 3 and 5 mL.min^{-1} display distorted peaks that tend to spread along the UF (vertical) dimension, as in the experiments without ODNP hyperpolarization (the effect is simply made more visible by the enhanced SNR).

It is concluded that 2D UF COSY experiments in continuous-flow are unfavorable at flow rates above 1 mL.min^{-1} as the time required for the spatial encoding as well as the signal acquisition are disturbed by the fast outflow of the sample from the detection zone which is difficult to quantify exactly due to the nature of the flow, regardless of applying ODNP hyperpolarization or not. This outflow issue can be tackled by using the interrupted-flow mode and separating the acquisition from the flow, which is discussed in the following section.

3.4. UF COSY ODNP in interrupted-flow

The results of the 2D UF COSY experiments with ODNP hyperpolarization in the interrupted-flow mode are shown Fig. 5. In this approach, one also waits for the polarization to reach a plateau in the detection cell after the microwaves are turned on. However, in this case, the 6-way valve is switched just before data acquisition. It can be seen that the 2D UF COSY NMR spectra obtained with this approach remain of high quality for all tested flow rates (up to 5 mL.min^{-1}). similar as in the thermal equilibrium case discussed in Section 3.2. To quantify the signal enhancements by applying ODNP hyperpolarization, the SNRs of the 2D UF COSY NMR spectra with ODNP hyperpolarization are compared to those achieved at thermal equilibrium, (see Fig. 6).

The SNRs displayed in Fig. 6 show that SNR enhancements are obtained for each signal throughout the studied flow rates. Detailed SNR enhancements obtained with 2D UF COSY in interrupted-flow are provided in Figure S5 in the Supporting Information. At a flow rate of 1 mL.min^{-1}, we observe a mean SNR enhancement of $\varepsilon = \mathbf{3.42 \pm 0.43}$ which is the largest SNR enhancement obtained in this study. However, by increasing the flow rate the SNR enhancement by ODNP hyperpolarization decreases. For a flow rate of 3 and 5 mL.min^{-1}, an average SNR enhancement of $\varepsilon = \mathbf{2.00 \pm 0.11}$ and $\varepsilon = \mathbf{2.67 \pm 0.30}$ are obtained, respectively. The signal enhancements of the corresponding 1D NMR experiments were also calculated resulting in the same trend as observed in the 2D UF COSY experiments. SNR enhancements of the 1D NMR experiments conducted in interrupted-flow are provided in the Supporting Information (Figure S4).

The limit of detection (LOD) of some 2D UF COSY experiments were estimated and are shown in the Supporting Information (Table S3 and Table S4). The LOD of the 2D UF COSY experiments under ODNP with an interrupted-flow of 1 mL.min^{-1} is 0.38 mol.L^{-1}. The LOD of the 2D UF COSY experiments at thermal equilibrium under static condition is 0.71 mol.L^{-1}. This means that, in this case, thanks to the sensitivity boost provided by flow ODNP hyperpolarization, we can detect concentrations 1.8 times lower than what is accessible with regular 2D UF COSY NMR.

In the case of interrupted-flow, acquisitions were launched simultaneously with the flow interruption. We can therefore expect that there are still molecular motions disturbing the spatial encoding of ultrafast 2D NMR and deteriorating the measured SNR. This hypothesis is validated by the fact that, at thermal equilibrium, the SNRs measured in interrupted-flow are all lower than the SNRs measured under static conditions. However, the SNR of the 2D UF COSY experiments with ODNP hyperpolarization are in a similar range as those obtained in the experiments at rest and at thermal equilibrium. This means that ODNP at least compensates for the loss of sensitivity induced by the residual motions of the sample. The 1 mL.min^{-1} ODNP interrupted-flow experiments provided SNRs all superior than the SNRs under static condition at thermal equilibrium. This means that ODNP compensates for the loss of sensitivity induced by the flow and provides further SNR enhancements.

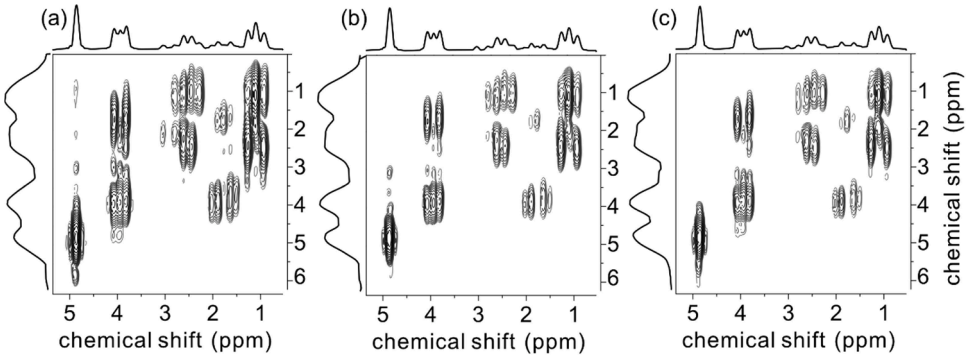

Fig. 5. 2D UF COSY NMR spectra of an equimolar mixture of propionaldehyde and 1,3-dioxane at **(a)** 1 mL.min^{-1}, **(b)** 3 mL.min^{-1} and **(c)** 5 mL.min^{-1} enhanced by ODNP hyperpolarization in interrupted-flow mode.

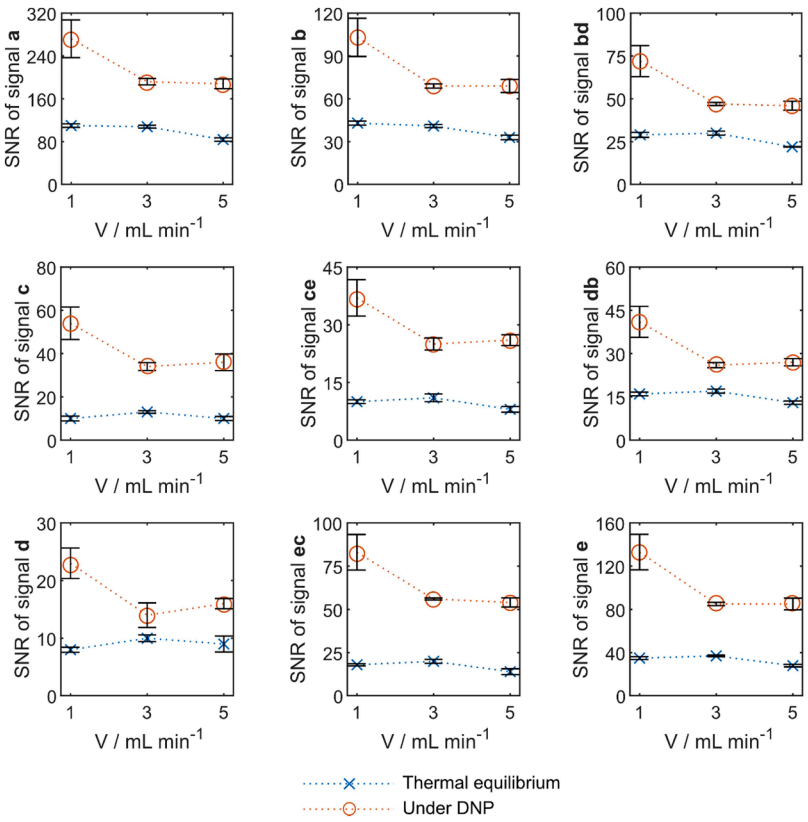

Fig. 6. Comparison of the SNRs obtained at thermal equilibrium and with ODNP hyperpolarization in interrupted-flow at the different flow rates (V). The comparison is carried out for the nine signals (the peak assignment is given in Fig. 2) present in the 2D UF COSY NMR spectra.

Additional information about the comparison of the results of the 2D UF COSY experiments and ODNP hyperpolarization with the results at static conditions are provided in the Supporting Information (see Figure S5).

The dependence of the signal enhancements on the flow rates may be rationalized by the longitudinal relaxation time constants T_1 of the two components. In flow ODNP, especially in this current setup, the net signal enhancement is a result of the hyperpolarization build-up in the ODNP probe, the relaxation during the transport from the fixed bed with the radical matrix to the detection zone, and the mixing of hyperpolarized and thermally polarized spins in the detection volume. The application of high flow rates reduces the hyperpolarization losses during the transfer to the detection zone. In contrast, a too high flow rate can lead to insufficient build-up of the hyperpolarization in the Halbach magnet as the corresponding residence time of the fluid on the fixed bed is too low. The relative contribution of these two effects depends on the T_1 values of the studied molecules. A shorter T_1 allows a rapid build-up of polarization in the Halbach magnet, but also requires a faster transfer to avoid losses due to relaxation: in this case a faster flow rate is favorable. Vice versa, a longer T_1 time requires an extended residence time on the radical matrix in order to achieve maximal hyperpolarization build-up, whereas T_1 relaxation is less detrimental during transfer (a lower flow rate is then favorable). Consequently, the optimum flow rate is dictated primarily by the time required to achieve sufficient hyperpolarization of the sample. In our study, the best SNR enhancement is observed when flow rate of 1 mL.min^{-1} is used, for both 1D and UF COSY experiments. This is consistent with the relatively long T_1 values for the molecules in the mixture, which were measured to be of about 10 s (see **SI**).

A comparison between the results of the 2D UF COSY experiments with those obtained from the corresponding 1D NMR experiments (see Figure S6 in the Supporting Information), shows that the signal enhancements obtained in the 2D UF COSY experiment case are comparatively lower. The 2D UF COSY experiment is expected to be more susceptible to in-flow and out-flow effects due to the longer duration of the pulse sequence, and it might be the case that more mixing of hyperpolarized and thermally polarized spins in the detection region occurs between the first 90° excitation and the acquisition block of UF COSY. However, the variation of the enhancement from one peak to another is qualitatively preserved between UF COSY and 1D experiments as this relies on the hyperfine interaction of a specific structural group with the radical matrix and the hyperpolarization losses due to T_1 relaxation of the specific groups during the transport time.

4. Conclusions

We have shown that UF COSY spectra can be acquired for a mixture of molecules hyperpolarized by flow ODNP. Good quality 2D NMR spectra were obtained in a single scan at flow rates of up to 1 mL.min^{-1} with continuous-flow acquisition, and 5 mL.min^{-1} using interrupted-flow acquisition. Mean SNR enhancements in the 2.00 – 3.37 range were obtained, and ODNP at least compensated for the sensitivity losses induced by high flow velocities. The choice of optimal acquisition mode (continuous or interrupted-flow) thus depends on the flow rate, while the choice of optimal flow rate depends in part on the longitudinal relaxation time constants. While the sample analyzed here did not evolve in time, in the context of process monitoring the choice of optimal flow rate would also depend on the kinetics of the process of interest. The demanding conditions of flow ODNP and UF 2D NMR are thus shown to be compatible in this example. This proof of concept is a first step towards using these methods to increase both the resolution and sensitivity of benchtop NMR spectroscopy for process monitoring applications. In the current state of the installation, the combination of 2D UF COSY and ODNP under flow conditions is limited for more resolute monitoring of simple evolving mixtures, with a non-negligible concentration of analytes, that can be hyperpolarized by ODNP. Further improvements (in hardware, for example) should be made to

enhance the capabilities of the technique, opening up new prospects for monitoring more complex processes.

CRediT authorship contribution statement

Joris Mandral: Writing – review & editing, Writing – original draft, Visualization, Validation, Resources, Methodology, Investigation, Data curation, Conceptualization. **Johnnie Phuong:** Writing – review & editing, Writing – original draft, Visualization, Validation, Resources, Methodology, Investigation, Data curation, Conceptualization. **Jonathan Farjon:** Writing – review & editing, Supervision, Funding acquisition, Conceptualization. **Patrick Giraudeau:** Writing – review & editing, Supervision, Funding acquisition, Conceptualization. **Kerstin Münnemann:** Writing – review & editing, Supervision, Project administration, Funding acquisition, Conceptualization. **Jean-Nicolas Dumez:** Writing – review & editing, Supervision, Project administration, Funding acquisition, Conceptualization.

Declaration of competing interest

The authors declare that they have no known competing financial interests or personal relationships that could have appeared to influence the work reported in this paper.

Acknowledgements

This work has received funding from the European Research Council under the European Union's Horizon 2020 research and innovation program (grant agreements no 814747/SUMMIT and 801774/DINAMIX) and the Region Pays de la Loire (ConnectTalent/HPNMR). Authors from CEISAM acknowledge the French National Infrastructure for Metabolomics and Fluxomics Metabo HUB-ANR-11-INBS-0010 (www.metabohub.fr) and the Corsaire metabolomics core facility (Biogenouest). We acknowledge Sarah Mross in the Laboratory of Engineering Thermodynamics of Kaiserslautern for her help in providing T1 values for the Supporting Information section. JM acknowledges the French ministry of higher education and research for funding his PhD thesis. JF warmly thanks his partner Sandrine Bouchet for unfailing assistances. Authors from Germany thank the German Research Foundation (DFG) for the financial support within the Collaborative Research Center SFB 1527 HyPERiON and the core facility INST 248/370–1.

Supplementary materials

Supplementary material associated with this article can be found, in the online version, at doi:10.1016/j.jmro.2025.100195.

Data availability

Data will be made available on request.

References

[1] K. Meyer, S. Kern, N. Zientek, G. Guthausen, M. Maiwald, Process control with compact NMR, TrAC Trends Anal. Chem. 83 (2016) 39–52, https://doi.org/10.1016/j.trac.2016.03.016.
[2] T.H. Rehm, Flow photochemistry as a tool in organic synthesis, Chem. – Eur. J. 26 (2020) 16952–16974, https://doi.org/10.1002/chem.202000381.
[3] H.-Y. Yu, S. Myoung, S. Ahn, Recent applications of Benchtop nuclear magnetic resonance spectroscopy, Magnetochemistry 7 (2021) 121, https://doi.org/10.3390/magnetochemistry7090121.
[4] M. Maiwald, H.H. Fischer, Y.-K. Kim, K. Albert, H. Hasse, Quantitative high-resolution on-line NMR spectroscopy in reaction and process monitoring, J. Magn. Reson. 166 (2004) 135–146, https://doi.org/10.1016/j.jmr.2003.09.003.
[5] M. Bazzoni, C. Lhoste, J. Bonnet, K.E. Konan, A. Bernard, P. Giraudeau, F. Felpin, J. Dumez, In-line multidimensional NMR monitoring of photochemical flow reactions, Chem. – Eur. J. 29 (2023) e202203240, https://doi.org/10.1002/chem.202203240.
[6] Y. Kharbanda, M. Urbańczyk, V.V. Zhivonitko, S. Mailhiot, M.I. Kettunen, V. Telkki, Sensitive, efficient and portable analysis of molecular exchange processes by hyperpolarized Ultrafast NMR, Angew. Chem. Int. Ed. 61 (2022) e202203957, https://doi.org/10.1002/anie.202203957.
[7] S.K. Küster, E. Danieli, B. Blümich, F. Casanova, High-resolution NMR spectroscopy under the fume hood, Phys. Chem. Chem. Phys. 13 (2011) 13172, https://doi.org/10.1039/c1cp21180c.
[8] F. Dalitz, M. Cudaj, M. Maiwald, G. Guthausen, Process and reaction monitoring by low-field NMR spectroscopy, Prog. Nucl. Magn. Reson. Spectrosc. 60 (2012) 52–70, https://doi.org/10.1016/j.pnmrs.2011.11.003.
[9] E. Danieli, J. Perlo, A.L.L. Duchateau, G.K.M. Verzijl, V.M. Litvinov, B. Blümich, F. Casanova, On-line monitoring of chemical reactions by using bench-top nuclear magnetic resonance spectroscopy, ChemPhysChem 15 (2014) 3060–3066, https://doi.org/10.1002/cphc.201402049.
[10] J. Mitchell, L.F. Gladden, T.C. Chandrasekera, E.J. Fordham, Low-field permanent magnets for industrial process and quality control, Prog. Nucl. Magn. Reson. Spectrosc. 76 (2014) 1–60, https://doi.org/10.1016/j.pnmrs.2013.09.001.
[11] T. Maschmeyer, L.P.E. Yunker, J.E. Hein, Quantitative and convenient real-time reaction monitoring using stopped-flow benchtop NMR, React. Chem. Eng. 7 (2022) 1061–1072, https://doi.org/10.1039/D2RE00048B.
[12] M. Rodriguez-Zubiri, F.-X. Felpin, Analytical tools integrated in continuous-flow reactors: which one for what? Org. Process Res. Dev. 26 (2022) 1766–1793, https://doi.org/10.1021/acs.oprd.2c00102.
[13] F. Dalitz, M. Cudaj, M. Maiwald, G. Guthausen, Process and reaction monitoring by low-field NMR spectroscopy, Prog. Nucl. Magn. Reson. Spectrosc. 60 (2012) 52–70, https://doi.org/10.1016/j.pnmrs.2011.11.003.
[14] E. Danieli, J. Perlo, A.L.L. Duchateau, G.K.M. Verzijl, V.M. Litvinov, B. Blümich, F. Casanova, On-line monitoring of chemical reactions by using bench-top nuclear magnetic resonance spectroscopy, ChemPhysChem 15 (2014) 3060–3066, https://doi.org/10.1002/cphc.201402049.
[15] M.V. Silva Elipe, R.R. Milburn, Monitoring chemical reactions by low-field benchtop NMR at 45 MHz: pros and cons, Magn. Reson. Chem. 54 (2016) 437–443, https://doi.org/10.1002/mrc.4189.
[16] K. Meyer, S. Kern, N. Zientek, G. Guthausen, M. Maiwald, Process control with compact NMR, TrAC Trends Anal. Chem. 83 (2016) 39–52, https://doi.org/10.1016/j.trac.2016.03.016.
[17] P. Giraudeau, F.-X. Felpin, Flow reactors integrated with in-line monitoring using benchtop NMR spectroscopy, React. Chem. Eng. 3 (2018) 399–413, https://doi.org/10.1039/C8RE00083B.
[18] A. Friebel, E. Von Harbou, K. Münnemann, H. Hasse, Reaction monitoring by benchtop NMR spectroscopy using a novel stationary flow reactor setup, Ind. Eng. Chem. Res. 58 (2019) 18125–18133, https://doi.org/10.1021/acs.iecr.9b03048.
[19] M. Leutzsch, A.J. Sederman, L.F. Gladden, M.D. Mantle, In situ reaction monitoring in heterogeneous catalysts by a benchtop NMR spectrometer, Magn. Reson. Imag. 56 (2019) 138–143, https://doi.org/10.1016/j.mri.2018.09.006.
[20] A. Friebel, E. Von Harbou, K. Münnemann, H. Hasse, Online process monitoring of a batch distillation by medium field NMR spectroscopy, 2021. https://doi.org/10.31219/osf.io/fuy3e.
[21] M.V. Silva Elipe, R.R. Milburn, Monitoring chemical reactions by low-field benchtop NMR at 45 MHz: pros and cons, Magn. Reson. Chem. 54 (2016) 437–443, https://doi.org/10.1002/mrc.4189.
[22] D. Gołowicz, K. Kazimierczuk, M. Urbańczyk, T. Ratajczyk, Monitoring hydrogenation reactions using Benchtop 2D NMR with extraordinary sensitivity and spectral resolution, ChemistryOpen 8 (2019) 196–200, https://doi.org/10.1002/open.201800294.
[23] J. Farjon, How to face the low intrinsic sensitivity of 2D heteronuclear NMR with fast repetition techniques: go faster to go higher!, Magn. Reson. Chem. 55 (2017) 883–892, https://doi.org/10.1002/mrc.4596.
[24] M. Bazzoni, B. Lorandel, C. Lhoste, P. Giraudeau, J.-N. Dumez, Fast 2D NMR for reaction and process monitoring, in: J.-N. Dumez, P. Giraudeau (Eds.), Fast 2D Solut.-State NMR, 1st ed., The Royal Society of Chemistry, 2023: pp. 251–283. https://doi.org/10.1039/BK9781839168062-00251.
[25] B. Luy, Fast pulsing 2D NMR methods, in: J.-N. Dumez, P. Giraudeau (Eds.), Fast 2D Solut.-State NMR Concepts Appl., The Royal Society of Chemistry, 2023: p. 0. https://doi.org/10.1039/BK9781839168062-00060.
[26] P. Giraudeau, L. Frydman, Ultrafast 2D NMR: an emerging tool in analytical spectroscopy, Annu. Rev. Anal. Chem. 7 (2014) 129–161, https://doi.org/10.1146/annurev-anchem-071213-020208.
[27] C. Lhoste, B. Lorandel, C. Praud, A. Marchand, R. Mishra, A. Dey, A. Bernard, J.-N. Dumez, P. Giraudeau, Ultrafast 2D NMR for the analysis of complex mixtures, Prog. Nucl. Magn. Reson. Spectrosc. 130–131 (2022) 1–46, https://doi.org/10.1016/j.pnmrs.2022.01.002.
[28] B. Gouilleux, J. Marchand, B. Charrier, G.S. Remaud, P. Giraudeau, High-throughput authentication of edible oils with benchtop ultrafast 2D NMR, Food Chem 244 (2018) 153–158, https://doi.org/10.1016/j.foodchem.2017.10.016.
[29] B. Gouilleux, B. Charrier, E. Danieli, J.-N. Dumez, S. Akoka, F.-X. Felpin, M. Rodriguez-Zubiri, P. Giraudeau, Real-time reaction monitoring by ultrafast 2D NMR on a benchtop spectrometer, Analyst 140 (2015) 7854–7858, https://doi.org/10.1039/C5AN01998B.
[30] C. Lhoste, M. Bazzoni, J. Bonnet, A. Bernard, F.-X. Felpin, P. Giraudeau, J.-N. Dumez, Broadband ultrafast 2D NMR spectroscopy for online monitoring in continuous flow, Analyst 148 (2023) 5255–5261, https://doi.org/10.1039/D3AN01165H.
[31] B. Gouilleux, B. Charrier, S. Akoka, F.-X. Felpin, M. Rodriguez-Zubiri, P. Giraudeau, Ultrafast 2D NMR on a benchtop spectrometer: applications and perspectives, TrAC Trends Anal. Chem. 83 (2016) 65–75, https://doi.org/10.1016/j.trac.2016.01.014.

[32] M. Bazzoni, C. Lhoste, J. Bonnet, K.E. Konan, A. Bernard, P. Giraudeau, F. Felpin, J. Dumez, In-line multidimensional NMR monitoring of photochemical flow reactions, Chem. – Eur. J. 29 (2023) e202203240, https://doi.org/10.1002/chem.202203240.
[33] M. Gal, M. Mishkovsky, L. Frydman, Real-time monitoring of chemical transformations by ultrafast 2D NMR spectroscopy, J. Am. Chem. Soc. 128 (2006) 951–956, https://doi.org/10.1021/ja0564158.
[34] L. Frydman, D. Blazina, Ultrafast two-dimensional nuclear magnetic resonance spectroscopy of hyperpolarized solutions, Nat. Phys. 3 (2007) 415–419, https://doi.org/10.1038/nphys597.
[35] C. Praud, V. Ribay, A. Dey, B. Charrier, J. Mandral, J. Farjon, J.-N. Dumez, P. Giraudeau, Optimization of heteronuclear ultrafast 2D NMR for the study of complex mixtures hyperpolarized by dynamic nuclear polarization, Anal. Methods 15 (2023) 6209–6219, https://doi.org/10.1039/D3AY01681A.
[36] P. Štěpánek, C. Sanchez-Perez, V.-V. Telkki, V.V. Zhivonitko, A.M. Kantola, High-throughput continuous-flow system for SABRE hyperpolarization, J. Magn. Reson. 300 (2019) 8–17, https://doi.org/10.1016/j.jmr.2019.01.003.
[37] D. Gołowicz, K. Kazimierczuk, M. Urbańczyk, T. Ratajczyk, Monitoring hydrogenation reactions using Benchtop 2D NMR with extraordinary sensitivity and spectral resolution, ChemistryOpen 8 (2019) 196–200, https://doi.org/10.1002/open.201800294.
[38] K. Jeong, S. Min, H. Chae, S.K. Namgoong, Monitoring of hydrogenation by benchtop NMR with parahydrogen-induced polarization, Magn. Reson. Chem. 57 (2019) 44–48, https://doi.org/10.1002/mrc.4791.
[39] O. Semenova, P.M. Richardson, A.J. Parrott, A. Nordon, M.E. Halse, S.B. Duckett, Reaction monitoring using SABRE-hyperpolarized benchtop (1 T) NMR spectroscopy, Anal. Chem. 91 (2019) 6695–6701, https://doi.org/10.1021/acs.analchem.9b00729.
[40] H.C. Dorn, T.E. Glass, R. Gitti, K.H. Tsai, Transfer of1H and13C dynamic nuclear polarization from immobilized nitroxide radicals to flowing liquids, Appl. Magn. Reson. 2 (1991) 9–27, https://doi.org/10.1007/BF03166265.
[41] M.D. Lingwood, T.A. Siaw, N. Sailasuta, B.D. Ross, P. Bhattacharya, S. Han, Continuous flow Overhauser dynamic nuclear polarization of water in the fringe field of a clinical magnetic resonance imaging system for authentic image contrast, J. Magn. Reson. 205 (2010) 247–254, https://doi.org/10.1016/j.jmr.2010.05.008.
[42] M.D. Lingwood, A.J. Sederman, M.D. Mantle, L.F. Gladden, S. Han, Overhauser dynamic nuclear polarization amplification of NMR flow imaging, J. Magn. Reson. 216 (2012) 94–100, https://doi.org/10.1016/j.jmr.2012.01.007.
[43] V. Denysenkov, M. Terekhov, R. Maeder, S. Fischer, S. Zangos, T. Vogl, T.F. Prisner, Continuous-flow DNP polarizer for MRI applications at 1.5 T, Sci. Rep. 7 (2017) 44010, https://doi.org/10.1038/srep44010.
[44] R. Kircher, H. Hasse, K. Münnemann, High flow-rate benchtop NMR spectroscopy enabled by continuous overhauser DNP, Anal. Chem. 93 (2021) 8897–8905, https://doi.org/10.1021/acs.analchem.1c01118.
[45] R. Kircher, S. Mross, H. Hasse, K. Münnemann, Functionalized controlled porous glasses for producing radical-free hyperpolarized liquids by Overhauser DNP, Molecules 27 (2022) 6402, https://doi.org/10.3390/molecules27196402.
[46] T.J. Keller, A.J. Laut, J. Sirigiri, T. Maly, High-resolution Overhauser dynamic nuclear polarization enhanced proton NMR spectroscopy at low magnetic fields, J. Magn. Reson. 313 (2020) 106719, https://doi.org/10.1016/j.jmr.2020.106719.
[47] J.L. Yoder, P.E. Magnelind, M.A. Espy, M.T. Janicke, Exploring the limits of Overhauser dynamic nuclear polarization (O-DNP) for portable magnetic resonance detection of low γ nuclei, Appl. Magn. Reson. 49 (2018) 707–724, https://doi.org/10.1007/s00723-018-1014-1.
[48] J. Phuong, B. Salgado, T. Labusch, H. Hasse, K. Münnemann, Overhauser dynamic nuclear polarization enables single scan benchtop 13C NMR spectroscopy in continuous-flow, Anal. Chem. (2025), https://doi.org/10.1021/acs.analchem.4c03985.
[49] Y. Shrot, L. Frydman, The effects of molecular diffusion in ultrafast two-dimensional nuclear magnetic resonance, J. Chem. Phys. 128 (2008) 164513, https://doi.org/10.1063/1.2890969.
[50] P. Giraudeau, S. Akoka, Sensitivity losses and line shape modifications due to molecular diffusion in continuous encoding ultrafast 2D NMR experiments, J. Magn. Reson. 195 (2008) 9–16, https://doi.org/10.1016/j.jmr.2008.08.001.
[51] P. Giraudeau, S. Akoka, Sources of sensitivity losses in ultrafast 2D NMR, J. Magn. Reson. 192 (2008) 151–158, https://doi.org/10.1016/j.jmr.2008.02.007.
[52] M.D. Lingwood, A.J. Sederman, M.D. Mantle, L.F. Gladden, S. Han, Overhauser dynamic nuclear polarization amplification of NMR flow imaging, J. Magn. Reson. 216 (2012) 94–100, https://doi.org/10.1016/j.jmr.2012.01.007.
[53] A.M.R. Hall, J.C. Chouler, A. Codina, P.T. Gierth, J.P. Lowe, U. Hintermair, Practical aspects of real-time reaction monitoring using multi-nuclear high resolution FlowNMR spectroscopy, Catal. Sci. Technol. 6 (2016) 8406–8417, https://doi.org/10.1039/C6CY01754A.